Schizophrenia Bulletin vol. 41 no. 6 pp. 1326–1335, 2015
doi:10.1093/schbul/sbv060
Advance Access publication May 4, 2015

Disintegration of Sensorimotor Brain Networks in Schizophrenia

Tobias Kaufmann*[,1], Kristina C. Skåtun[1], Dag Alnæs[2], Nhat Trung Doan[1], Eugene P. Duff[3], Siren Tønnesen[1], Evangelos Roussos[3], Torill Ueland[1,2], Sofie R. Aminoff[1,4], Trine V. Lagerberg[1], Ingrid Agartz[1,5], Ingrid S. Melle[1], Stephen M. Smith[3], Ole A. Andreassen[1], and Lars T. Westlye[1,2]

[1]NORMENT, KG Jebsen Centre for Psychosis Research, Division of Mental Health and Addiction, Oslo University Hospital & Institute of Clinical Medicine, University of Oslo, Oslo, Norway; [2]Department of Psychology, University of Oslo, Oslo, Norway; [3]FMRIB Centre, Nuffield Department of Clinical Neurosciences, University of Oxford, Oxford, UK; [4]Department of Specialized Inpatient Treatment, Division of Mental Health Services, Akershus University Hospital, Oslo, Norway; [5]Department of Psychiatric Research, Diakonhjemmet Hospital, Oslo, Norway

*To whom correspondence should be addressed; NORMENT, KG Jebsen Centre for Psychosis Research, Oslo University Hospital, Kirkeveien 166, 0407 Oslo, Norway; tel: +47 23 02 73 50, fax: +47 23 02 73 33, e-mail: tobias.kaufmann@medisin.uio.no

Background: **Schizophrenia is a severe mental disorder associated with derogated function across various domains, including perception, language, motor, emotional, and social behavior. Due to its complex symptomatology, schizophrenia is often regarded a disorder of cognitive processes. Yet due to the frequent involvement of sensory and perceptual symptoms, it has been hypothesized that functional disintegration between sensory and cognitive processes mediates the heterogeneous and comprehensive schizophrenia symptomatology.** ***Methods:*** **Here, using resting-state functional magnetic resonance imaging in 71 patients and 196 healthy controls, we characterized the standard deviation in BOLD (blood-oxygen-level-dependent) signal amplitude and the functional connectivity across a range of functional brain networks. We investigated connectivity on the edge and node level using network modeling based on independent component analysis and utilized the brain network features in cross-validated classification procedures.** ***Results:*** **Both amplitude and connectivity were significantly altered in patients, largely involving sensory networks. Reduced standard deviation in amplitude was observed in a range of visual, sensorimotor, and auditory nodes in patients. The strongest differences in connectivity implicated within-sensorimotor and sensorimotor-thalamic connections. Furthermore, sensory nodes displayed widespread alterations in the connectivity with higher-order nodes. We demonstrated robustness of effects across subjects by significantly classifying diagnostic group on the individual level based on cross-validated multivariate connectivity features.** ***Conclusion:*** **Taken together, the findings support the hypothesis of disintegrated sensory and cognitive processes in schizophrenia, and the foci of effects emphasize that targeting the sensory and perceptual domains may be key to enhance our understanding of schizophrenia pathophysiology.**

Keywords: functional imaging/machine learning/resting state/schizophrenia

Introduction

Schizophrenia is a major cause of disability, affecting more than 26 million people worldwide.[1] It is characterized by abnormalities in several domains, including perception, language, motor, emotional processing, and social behavior, yet the phenomenology may be as diverse that 2 patients may not share one common symptom.[2]

With a profound understanding of the schizophrenia pathophysiology lacking,[3] a large number of neuroimaging studies have provided evidence for the *dysconnectivity hypothesis*, implying brain functional disintegration in the pathophysiology.[4,5] Available evidence largely converges on decreased connectivity in schizophrenia as well as on the involvement of prefrontal regions, but the exact brain regions involved and the characteristics of the dysconnectivity vary considerably across studies,[6] suggesting diverse brain connectivity profiles in schizophrenia.[7] This inconsistency may in part be explained by small sample sizes, diversity in age, gender and medication status, different analytical approaches, and true pathophysiological heterogeneity.[6]

Due to consistent reports of cognitive impairments,[8,9] avolition, and the involvement of higher-order brain regions,[6] schizophrenia has been regarded a disorder of higher-order, cognitive functions.[10] Yet the clear involvement of visual, auditory, and sensorimotor processes in the symptomatology (eg, auditory hallucinations) suggests impaired function and integration of bottom-up and top-down brain networks.[10] Indeed, whereas auditory hallucinations have been regarded as a relatively common perceptual phenomenon (bottom-up), being overwhelmed

by "voices," which is a characteristic feature of schizophrenia, reflects an additional failure of inhibitory control (top-down).[11] Consequently, dissecting the mechanisms of psychotic disorders requires increased knowledge about the interplay between and the functioning within sensory and cognitive brain processes. Such interplay and functioning can be studied using temporal correlation of BOLD (blood-oxygen-level-dependent) signals between regions (functional connectivity [FC]) as well as the signal variance within regions. The latter was proven a sensitive measure of brain integrity, revealing patterns that are not captured by mean-based analyses.[12,13]

Here, we assess the standard deviation (SD) in amplitude (SDSA) and the FC of a range of large-scale brain networks using resting-state functional magnetic resonance imaging (rfMRI) in 267 individuals including 71 patients diagnosed with broad schizophrenia spectrum disorders. By complementary data-driven definition of brain network nodes, network modeling, and a combination of uni- and multivariate statistics, we probe brain connectivity features on the edge and node level. Utilizing machine learning for classification allows us to assess the sensitivity and specificity of the features.

Based on previous findings, we anticipated amplitude differences[14] in addition to mostly reduced connectivity[6] in patients compared with controls. More specifically, given the significant involvement of sensory and perceptual processes in the symptomatology and the hypothesis that schizophrenia is characterized by disintegration of bottom-up and top-down processes,[10] we hypothesized connectivity and amplitude alterations in visual, auditory, and motor cortices, and particularly in their integration with frontal brain regions.

Materials and Methods

Sample and Ethical Approval

We included 71 patients diagnosed with broad schizophrenia spectrum disorders (age range: 18.1–53.4 years, mean age: 28.2 years, 59.2% males) and 196 healthy controls (age range: 17.5–46.2 years, mean age: 31.5 years, 58.2% males). Demographic and clinical information are summarized in Table 1. Patients were recruited from the hospital register for both in- and outpatients, whereas controls were randomly selected from the Norwegian population register from the same catchment area. All patients underwent a

Table 1. Demographic and Clinical Characteristics

Characteristics	Schizophrenia	Healthy Controls
Demographics		
Total number	$N = 71$	$N = 196$
Age (mean years ± SD)[a]	28.2 ± 7.8	31.5 ± 7.8
Gender (abs male, %)[b]	$N = 42$, 59.2%	$N = 114$, 58.2%
Handedness (% right)[c,d]	92.8%	87.6%
Symptom rating (mean ± SD)[e]		
Positive and Negative Syndrome Scale (PANSS) total score	58.1 ± 13.7	
PANSS general score	30.0 ± 6.8	
PANSS positive score	13.3 ± 4.9	
PANSS negative score	14.8 ± 5.0	
GAF symptom score	46.1 ± 14.0	
Global Assessment of Functioning (GAF) function score	47.0 ± 12.3	
Medication (abs, mean DDD ± SD)[f]		
First generation antipsychotics[g]	$N = 5$, 2.82 ± 3.3	
Second generation antipsychotics[g]	$N = 56$, 1.47 ± 2.0	
Antidepressiva	$N = 21$, 2.51 ± 4.2	
Antiepileptica	$N = 3$, 0.32 ± 0.2	
Substance/alcohol usage and smoking		
Substance abuse	$N = 1$, 1.4%	
Alcohol abuse	$N = 1$, 1.4%	
Substance addiction	$N = 12$, 16.9%	
Alcohol addiction	$N = 6$, 8.5%	
Smokers	$N = 40$, 56.3%	

Note: [a]Groups significantly different in age: $t = 3.1$, $P < .003$.
[b]Groups not significantly different in gender: $\chi^2 = 0.02$, $P = .9$.
[c]Groups not significantly different in handedness: $\chi^2 = 1.2$, $P = .27$.
[d]Incomplete handedness data from $N = 15$ (schizophrenia), $N = 11$ (healthy controls).
[e]Incomplete symptom scores from $N = 4$.
[f]DDD = defined daily dose. Incomplete medication record from $N = 9$. Three patients did not receive any of the listed medications.
[g]The patients were treated with the following antipsychotics (N, mean DDD ± SD): Amisulpride ($N = 3$, 1.58 ± 0.8), Aripirazole ($N = 15$, 0.82 ± 0.3), Chlorprothixene ($N = 1$, 1 ± 0), Clozapine ($N = 4$, 0.68 ± 0.7), Flupentixol ($N = 1$, 6.67 ± 0), Haloperidol ($N = 1$, 6.25 ± 0), Ievomepromazine ($N = 2$, 0.1 ± 0.1), Olanzapine ($N = 19$, 1.09 ± 0.6), Palliperidone ($N = 5$, 4.43 ± 5.7), Quetiapine ($N = 17$, 0.78 ± 0.6), Risperidone ($N = 9$, 0.71 ± 0.3).

clinical interview by trained clinicians and were diagnosed according to the Diagnostic and Statistical Manual of Mental Disorders, Fourth Edition. Subdiagnoses included schizophrenia ($N = 33$), schizoaffective disorder ($N = 12$), schizophreniform disorder ($N = 3$), and psychosis not otherwise specified ($N = 23$). General exclusion criteria were an intelligence quotient below 70, history of head trauma, or other neurological disorders. In addition, healthy controls were excluded if they had first-degree relatives with mental disorders or if they had any history of drug addiction. All scans were examined by a neuroradiologist to rule out severe brain pathology. All participants signed informed consent prior to enrollment. Appropriate ethical approval was obtained, and all procedures were in line with the declaration of Helsinki.

MRI Data Collection

MRI scans were obtained from a General Electric (Signa HDxt) 3.0T scanner with an 8-channel head coil at Oslo University Hospital. Functional data were acquired with a T2*-weighted 2D gradient echo planar imaging sequence with 203 volumes (repetition time [TR]: 2.638 s; echo time(TE): 30 ms; flip angle (FA): 90°; voxel size: 4 × 4 × 3 mm; slices: 45; field of view (FOV): 256 mm^2; duration: 553 s). To assure equilibrium was reached, we discarded the first 5 volumes (ie, 198 volumes used). In addition, a structural scan was acquired using a sagittal T1-weighted fast spoiled gradient echo sequence (TR: 7.8 s; TE: 2.956 ms; TI [inversion time]: 450 ms; FA: 12°; voxel size: 1.0 × 1.0 × 1.2 mm; slices: 170; FOV: 256 mm^2; duration: 428 s).

MRI Processing

fMRI data were processed on single-subject level using the FMRI Expert Analysis Tool from the FMRIB Software Library (FSL[15]), including spatial smoothing (FWHM [full width at half maximum] = 6 mm), high-pass filtering (90 s), motion correction (MCFLIRT[16]), and single-session independent component analysis (ICA) using MELODIC.[17] Supplementary table 1 provides an overview of in-scanner subject motion defined as the average root mean square of the displacement from one frame to its previous frame for each data set. None of the subjects was excluded based on these estimates. Instead, we used FIX[18] to identify and remove noise components (standard training set, threshold: 20), yielding a cleaned data set for each subject (Pruim et al[19], for verification of method).

We used automated brain segmentation (Freesurfer[20]) of the T1-weighted data to obtain brain masks used for co-registration to a standard coordinate system using FLIRT,[21] optimized using boundary-based registration[22] and FNIRT.[23] Next, using the temporal concatenation approach in MELODIC, we performed group-level ICAs with different model orders, estimating 20, 40, 60, and 80 components. Due to computational resources, group-level ICAs were based on a randomly selected subset of participants, matched for age and diagnosis (45 per group; not significantly different in age, $P = .54$). Next, using dual regression,[24] we estimated individual component spatial maps and corresponding time series for each subject and for each model order. All components were manually screened and components reflecting noise were discarded. Informed decision was based on thresholded spatial maps ($z > 4$, regional loci outside reasonable areas) as well as frequency decomposition of the components' time courses (shift toward high frequencies). The number of kept components per model order was d20: 14, d40: 28, d60: 38, and d80: 47.

Then, after regressing out the time series of the discarded components from the time series of the remaining components, we computed the temporal Pearson correlation coefficients between each component using FSLNets.[25] The resulting correlation matrices represent the FC matrices, from which we selected the most appropriate model order for subsequent analysis (see "Machine-Learning-Based Model Selection" section). In addition, we computed L1-regularized partial correlation matrices with a range of λ values as alternative measures of FC to test the robustness across methods. Furthermore, for each data set, we computed the SD of each component's time series as a measure of nodal strength using FSLNets.[25] We refer to this measure as standard deviation of signal amplitude (SDSA).

Machine-Learning-Based Model Selection

A commonly accepted method for selecting the most appropriate model order for ICA does not exist. To complement the data-driven analysis procedure, we compared various model orders in a machine-learning-based approach. For each model order, we trained a regularized linear discriminant analysis (shrinkage LDA[26,27]) classifier on the full set of edgewise correlation coefficients (half of the FC matrix) using leave-one-out (LOO) cross-validation. This resulted in a cross-validated estimate of classifier performance for each model order. We used the Matthews correlation coefficient (MCC[28,29]) to assess classifier performance as it accounts for imbalance in the number of subjects per group. The MCC can vary between −1 (all decisions wrong) and 1 (all decisions correct), with 0 indicating random classification. To investigate how well the model orders capture case-control differences, we performed permutation tests for each model order, by randomly permuting the diagnostic labels 10 000 times[30] and rerunning LOO-validated classification for each permutated data set.

Case-Control Differences in Functional Connectivity and Signal Amplitude

To facilitate functional characterization of the brain network nodes, we clustered components based on the

Euclidean distances of the temporal correlations using the linkage function in Matlab (The Mathworks Inc), as implemented in FSLNets.[25] This step is mainly for visualization purpose. Next, we investigated case-control differences running an analysis of covariance (ANCOVA) on the SDSA of each node and the strength of each edge and, lastly, utilized regularized LDA to estimate the robustness of the case-control differences on a single-subject level.

Analysis on Edge Level. For each edge in the connectivity matrix, we performed an ANCOVA to test for effects of diagnosis while accounting for age and sex. This entailed a large number of tests, thereby increasing the probability of false positives. To facilitate transparency, we applied 2 levels of alpha correction, the false discovery rate (FDR[31,32]) and a strict Bonferroni correction. FDR level was computed for each test separately with a FDR level $q = 0.05$ and a threshold based on the assumption of independence or positive dependence for all reported FDR corrections. Throughout the manuscript, we report raw P values to provide full transparency. From the ANCOVA table, we computed edgewise partial eta-squared effect sizes to estimate the strength of effects. Finally, we used the machine-learning approach described above to assess the reliability of edge effects. Both analyses, edgewise ANCOVA and classification, were also performed on the regularized partial correlation matrices.

Analysis on Node Level. We conducted 2 analyses on the node (component) level. First, to estimate the relative importance of each node's connectivity in the case-control classification, we iteratively ran the above-described machine-learning procedure for each of the 47 nodes based on their 46 edges to all other nodes only. To assess the reliability of the obtained classifier performances, we ran an additional permutation test with 10 000 iterations for every node, each implementing a full LOO validation. Second, we tested for group differences in the nodewise SDSA using ANCOVA, covarying for age and sex.

Results

Model Selection and Clustering

Classifier performance as evaluated by the MCC was significantly above chance for all model orders (d20: MCC = 0.343, $P < .0001$; d40: MCC = 0.280, $P = .0001$; d60: MCC = 0.342, $P = .0001$; d80: MCC = 0.344, $P < .0001$), indicating robust case-control differences across dimensionalities. Here, we selected d80 as model order for all analyses, as it reached highest MCC while also providing a reasonable anatomical separation of components. The clustering tree of the 47 independent components is depicted in figure 1A and 1B, for a detailed description of components, see supplementary figure 1 and supplementary table 2.

Case-Control Differences in Functional Connectivity and Signal Amplitude

Analysis on Edge Level. Figure 1C depicts effect sizes for all edges displaying significantly altered FC as obtained from the Pearson correlation matrices. The 5 strongest effects of diagnosis all involved sensorimotor nodes (ICs 5, 20, 36, and 18), 4 of which showed decreased connectivity in patients within sensorimotor edges and 1 displaying increased connectivity with the thalamus (all $P < .00005$). This pattern was also visible at the less conservative FDR threshold with 20 of the 32 significant edges linking to sensorimotor nodes (all $P < .0015$). Eight of the sensorimotor edge effects at FDR level were seen between sensorimotor nodes, yet there were also widespread alterations in connections to higher-order networks such as the dorsal attention network (IC 17–36) and default mode network (IC 1–18, IC 11–36, IC 11–18). Apart from sensorimotor effects, we found decreased connectivity within the dorsal attention network (IC 17–22), between dorsal attention network and default mode network (IC 22–11), and between the thalamus and the caudate (IC 39–24), among others. Altogether, effects appeared mostly due to decreased FC in patients (65.6% of the significant edges). For the various sets of (regularized) partial correlation matrices, ANCOVAs consistently revealed one edge between left and right postcentral gyrus surviving Bonferroni correction in all sets (IC 20–36). Supplementary figure 2 provides full details.

We further validated these effects in a multivariate classification analysis using LOO cross-validation. Based on the full set of edges from the Pearson correlation matrices, we classified between cases and controls with an MCC of 0.344 (raw accuracy: 75.3%, sensitivity: 47.9%, specificity: 85.2%). The obtained classification accuracy was highly above chance with none of the 10 000 label-permuted data sets resulting in better MCC (ie, $P < 10^{-4}$). The best classification result on regularized partial correlation matrices was obtained with $\lambda = 0.125$ (MCC: 0.41, raw accuracy: 77.9%, sensitivity: 50.7%, specificity: 87.8%). Supplementary table 3 compares classification accuracies obtained with each set of (regularized) partial correlation matrices.

Furthermore, because the patient group included a relatively large cohort of patients diagnosed with psychosis not otherwise specified, we ran LOO-based classification with these patients ($N = 23$) excluded. For full correlation matrices and regularized partial correlation matrices with high λ, classification accuracy improved due to an increase in specificity. Again the best result was obtained for $\lambda = 0.125$ (MCC: 0.47, raw accuracy: 84.4%, sensitivity: 50.0%, specificity: 92.8%; $\lambda = 0.15$ gave similar results). For nonregularized partial correlations and those with low λ, sensitivity largely decreased. Supplementary table 4 summarizes all results of this exclusion analysis.

Finally, in addition to LOO cross-validation, we performed 10 000 classifications on the full correlation matrices

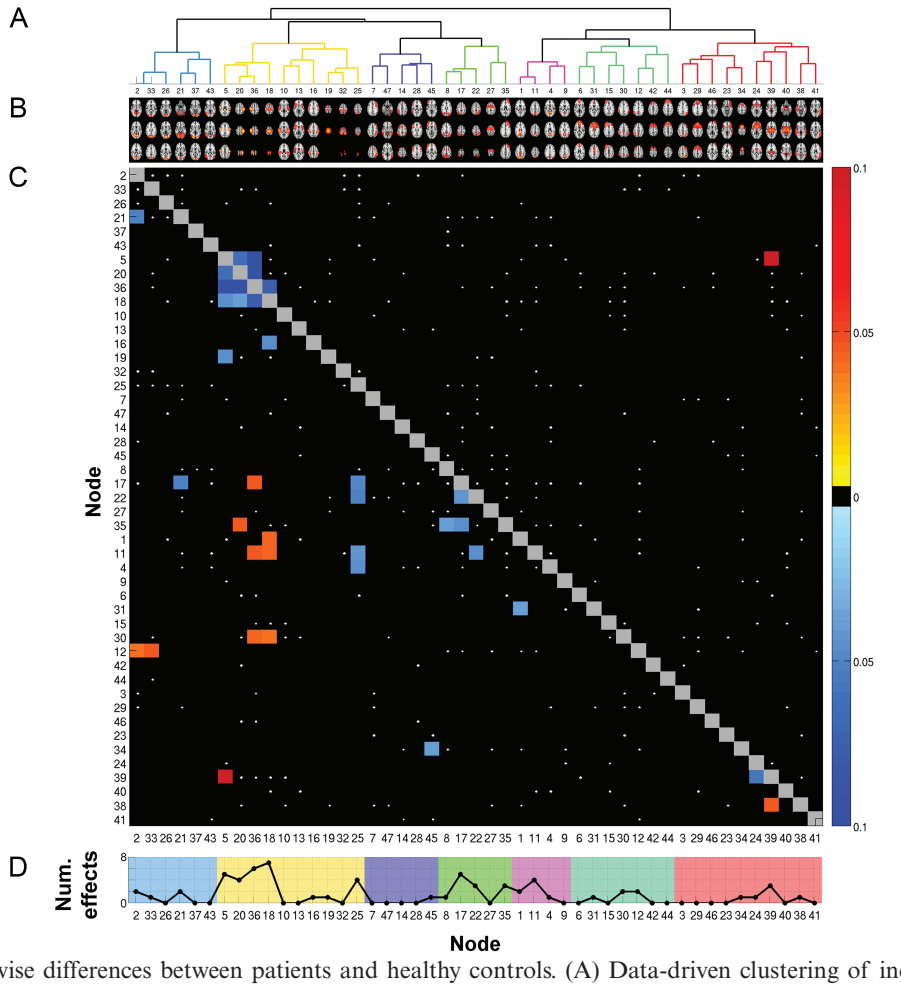

Fig. 1. Node- and edgewise differences between patients and healthy controls. (A) Data-driven clustering of independent components based on temporal correlations. (B) 47 independent components (model order 80; 33 noise components removed from the analysis). For a more detailed overview of components, see supplementary table 2 and supplementary figure 1. (C) Edgewise comparison of functional connectivity. Edges that show a significant effect of diagnosis are depicted as colored squares. The color represents partial eta-squared effect sizes that were accompanied with a sign to indicate the direction of the effect (toward blue: reduced connectivity in patients; toward red: increased connectivity in patients). All black squares are nonsignificant. White dots indicate effects at a nominal alpha level. To account for multiple comparisons, the lower half of the matrix displays only those edges that were significant at false discovery rate (FDR) level (21↓ + 11↑ significant edges with $P < .0015$). The upper half applies a Bonferroni correction (4↓ + 1↑ significant edges with $P < .00005$). (D) Absolute number of edge effects per node at FDR corrected alpha level (computed from panel C). The background color reflects the cluster a node belongs to (see panel A).

using a random split approach with 75% of data as training and 25% as test set. Supplementary figure 3 summarizes the results. Briefly, average classification performance closely resembles the LOO-based results (MCC: 0.34, raw accuracy: 75.8%, sensitivity: 46.5%, specificity: 86.0%).

Analysis on Node Level. Figure 1D summarizes the above-described univariate edge effects on the node level. For a closer investigation of the involvement of each individual node, we performed several further analyses on the node level. First, we classified between cases and controls using only edges of a single node (46 features) and validated each node's MCC against an empirical null distribution generated across 10 000 permutations, see figure 2. The 10 nodes significant at Bonferroni level (MCC range: 0.24–0.36, all $P < .001$) included 1 visual (IC 33), 5 sensorimotor (ICs 5, 20, 36, 18, 25), 1 dorsal attention (IC 17), 2 frontoparietal (IC 30, IC 34), and 1 thalamic node (IC 39). For one sensorimotor component (postcentral gyrus, IC 36), MCC obtained from just the 46 corresponding edges was higher than the MCC obtained on the full set of 1081 features. Supplementary table 6 provides full details on nodewise classification. Second, we compared nodewise SDSA across groups. As shown in figure 3, 11 nodes displayed reduced SDSA in patients significant at a Bonferroni level, involving visual (ICs 2, 33, 26, 21, 37), sensorimotor (ICs 5, 20, 36, 18), auditory (IC 10), and default mode (IC 11) network nodes (all $P < .001$, $\eta_P^2 = .05 - .08$).

Associations to Medication, Symptom Scores, and Substance Use. We investigated effects of medication,

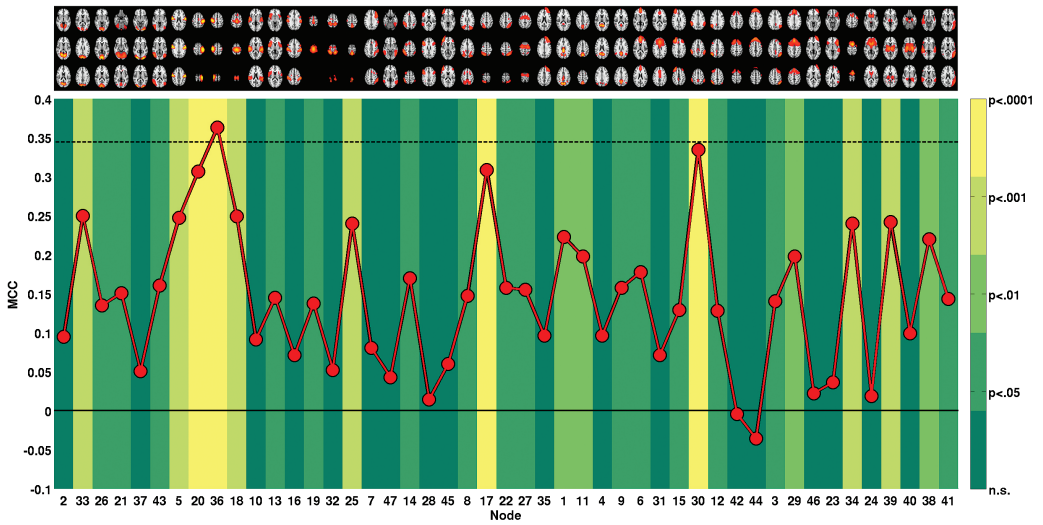

Fig. 2. Classification based on the 46 edges of each single node. The red line depicts obtained Matthews correlation coefficient (MCC). The solid black line indicates chance level (MCC = 0) and the dashed black line indicates MCC level achieved with full set of features (all 1081 edges). The color in the background of each node indicates the level of significance obtained from 10 000 permutation tests per node. For details, see supplementary table 6.

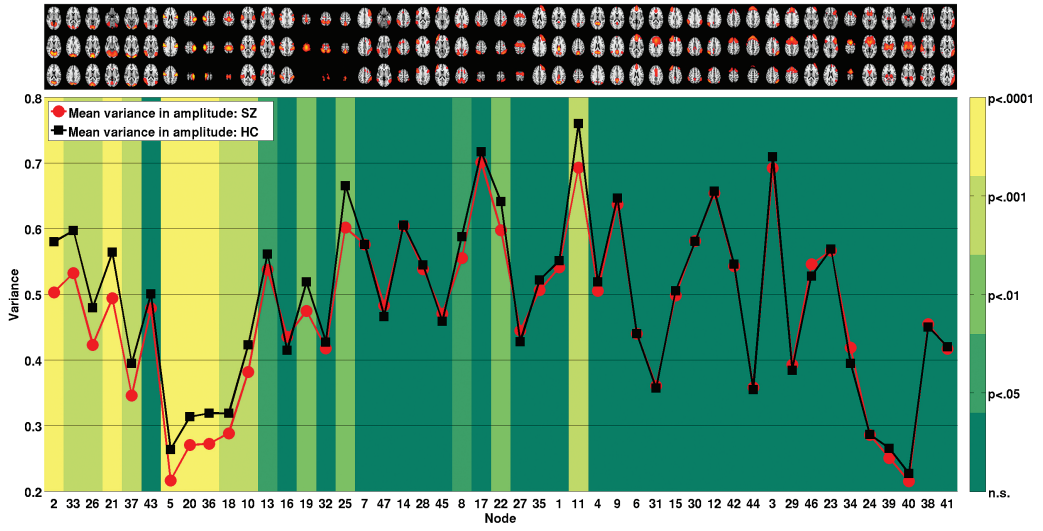

Fig. 3. Comparison of mean standard deviation in signal amplitude. The red and black lines depict mean SD of time series within patients and controls, respectively. The color in the background of each node indicates the level of significance of an analysis of covariance testing for differences between schizophrenia and healthy controls while accounting for age and gender.

symptoms, and substance use on FC and nodal SDSA within the patient group using ANCOVAs, accounting for age and gender. The results are provided in full detail in the supplementary material. Briefly, none of the edges (FC) and nodes (SDSA), showing a main effect of diagnosis, was significantly affected by either of the measures (defined daily dose of antipsychotic treatment, PANSS, GAF, substance addiction, smoking).

Motion as a Potential Confounder of Results

Patients showed significantly more in-scanner motion ($t = -3.9$, $P < .0001$), and FIX removed a significantly higher proportion of noise components from the patient group ($t = -2.2$, $P < .05$ and also removed more of the variance from the raw fMRI data, both in terms of absolute and relative variance [both $t = -2.8$, $P < .05$]). Proportion of noise removed was significantly correlated with amount of subject motion ($r = .52$, $P <$ 1e-19 across groups, $r = .53$, $P <$ 1e-05 within patient group, $r = .53$, $P <$ 1e-14 within control group). Supplementary table 5 provides additional descriptive statistics on FIX cleaning and supplementary figure 4 illustrates the impact of FIX cleaning on the voxel level, both within and across groups.

In addition to the use of FSL's FIX algorithm for data cleaning, we assessed the possible confounding effects of motion by including in-scanner subject motion as an

additional covariate in the ANCOVA models. Effect sizes with motion included in the model were significantly correlated to the above-reported effect sizes for both nodal SDSA (r = .42, P < .01) and edgewise connectivity analysis (r = .96, P < .00001, Pearson correlations). The number of significantly altered edges in connectivity analysis based on Pearson correlations decreased to 12 at FDR (alpha level decreased to alpha < .0005; IC 2–21, 5–20, 5–36, 5–39, 11–22, 17–35, 17–36, 18–36, 20–36, 22–25, 24–39, 38–39) and 3 at Bonferroni level (IC 5–36, 5–39, 20–36) when accounting for motion, yet all but one (P = .02, IC 4–25) of those edges that were no longer significant were still at the border of significance (maximum P = .006). Finally, for SDSA analysis, 4 of the 11 significant nodes remained significant at Bonferroni level when accounting for motion, yet all but one (IC 10: P = .06) were still significant at an FDR level of P < .011.

To investigate if motion might have a selective impact on connectivity depending on edges distance,[33] we conducted for each group an ANCOVA testing for main effect of motion on FC, while accounting for age and gender. Partial eta-squared effect sizes of the ANCOVA did not correlate with the Euclidean distance of the edges, neither for controls (r = .008, P = .8) nor for patients (r = −.004, P= .9).

Discussion

We have shown widespread brain FC and amplitude differences between patients with broad schizophrenia spectrum disorders and healthy controls using rfMRI and network modeling. We observed significant differences on edge and node level, indicating comprehensive system-level brain network dysfunctions in schizophrenia. A range of analyses on amplitude (SDSA) and connectivity converged on particularly strong effects in sensory, somatosensory, and motor nodes. These findings question the notion of schizophrenia as primarily a cognitive disorder and support that symptoms may in fact rather reflect cumulative cascade impairments originating in sensory and perceptual dysfunctions, in combination with failed integration between lower- and higher-order processes.[10,11] These novel findings will be discussed in detail below.

Connectivity and Amplitude Effects Largely Involve Sensory Nodes

The finding that sensorimotor nodes were largely involved across analyses is in line with previous reports of premotor and motor cortex dysfunction[34] and the presence of motor symptoms in nonmedicated patients with schizophrenia.[35,36] For analyses on various regularized partial correlations, one edge between the right and left postcentral gyri consistently remained significant, suggesting that most of the above-reported effects may be partly mediated by third-party regions. The postcentral gyrus has been repeatedly found to show reduced gray matter density in schizophrenia,[37] and as outlined recently, its reduced connectivity plays a central role in early-onset schizophrenia.[38]

Our sensorimotor findings were accompanied by reduced SDSA in visual nodes as well as altered connectivity in edges involving visual nodes. This is in line with previous studies documenting sensory and perceptual deficits in various domains from early-stage processing to cognitive stimulus interpretation.[39,40] The strong sensory involvement overlaps with findings from electroencephalogram studies, associating schizophrenia with a broad range of sensory deficits reflected among various event-related potentials (eg, reduced pre-pulse inhibition (PPI), MMN [mismatch negativity], P1, P3).[40]

Our data support both focal (within sensorimotor/visual nodes) and distal (between sensorimotor/visual and thalamus/higher-order nodes) connectivity differences in schizophrenia, including edges implicating dorsal attention, default mode, frontoparietal, and thalamus nodes. The thalamo-cortical functional disintegration in schizophrenia is in line with the prominent role of the thalamus in relaying and coordinating information between various cortical sources, including perceptual and motor processes, and supports a role of altered thalamus connectivity in the pathophysiology.[41,42] Its increased connectivity to sensorimotor networks is in line with recent investigations of thalamo-cortical disturbances in schizophrenia,[14,43,44] and may support the notion of schizophrenia being a neurodevelopmental disorder,[3] because modulation of thalamo-sensorimotor connectivity has been associated with brain maturation pointing to a strong over-connectivity in children.[44,45]

All significant differences in node amplitude were due to reduced SDSA in patients. This is inconsistent with a recent report showing increased voxelwise variance in schizophrenia,[14] yet is in line with the reasoning that variability is crucial for neural systems to transition between multiple functional states,[46] with greater variability generally reflecting superior brain functioning.[12,13] Reduced variance may (among others) reflect decreased FC, hampering the adaptability of the neural system.[13,47,48] The sensorimotor nodes showing a significant reduction in SDSA in our study also displayed significant connectivity alterations. However, reduced SDSA in visual and auditory nodes did not coincide with connectivity alterations in several of these nodes.

Robustness of Results and Future Perspectives

The current effects appeared relatively robust on single-subject level, as validated using machine learning and cross-validation. Using the full set of edges, we reliably discriminated between cases and controls with classification performance highly above chance. Interestingly, the edges of a single

node (IC 36, postcentral gyrus) were sufficient to reach similar level of performance. However, the sensitivity estimates from the classification analyses do not support a direct clinical application. It might be improved when including a larger, well-balanced sample with respect to subdiagnoses and employing an alternative diagnostic nosology based on a dimensional symptom-based perspective.[49] With respect to robustness across subjects, the cross-validation results show initial promise for a future utilization of neuroimaging markers in clinical contexts as a complement to clinical interviews. Using similar ICA-based network features has recently proven reliable for classification of mental states.[50]

Limitations

As for any study using MRI, we cannot fully rule out that our findings are influenced by subject motion. Yet we addressed this issue to the best of our capabilities, including ICA and machine-learning-based data cleaning (FIX[18]) in addition to regressing out motion parameters and incorporation of relative motion as a covariate in statistical analysis. FIX removed a significantly higher proportion of noise components from the patient group and the proportion of noise removed was significantly correlated with motion, both within and across groups. The reliability of FIX cleaning with respect to network reproducibility has recently been verified.[19] Furthermore, our main results of altered sensorimotor connectivity, both within sensorimotor nodes and to the thalamus, were unaffected when including motion as a covariate. Taken together, we are thus confident that the main effects reported in this article cannot be explained by motion.

Our analysis pipeline did not include a regression of the global signal, in line with studies using similar approaches,[24,51] and the result of a recent evaluation on the benefits of global signal regression (GSR).[19] Considering that the global signal likely contains both signal and noise, GSR decreases signal of interest.[19] We thus used FIX to remove noise components selectively. In addition, global signal will have minimal influence on partial correlation network matrices, which characterize the extent of unique shared signal between pairs of nodes.

Furthermore, medication effects could have affected our results. This is difficult to assess due to the colinearity between diagnosis and medication status. Medication effects should thus be assessed individually by an appropriately designed study (randomized controlled trial) to control the range of confounders. However, it has been shown that sensorimotor effects in schizophrenia are present independent of medication,[52] attenuating the probability of medication effects confounding our main results. Finally, our sample included 23 patients diagnosed with psychosis not otherwise specified. Although these patients fall into the broad schizophrenia spectrum disorders category, their inclusion may hamper both the generalization and diagnostic specificity of our results. We addressed this by an additional analysis with these patients excluded. As a result, specificity increased (the classifier improved on identifying controls). For partial correlation matrices with low λ, the increase in specificity was accompanied by a decrease in sensitivity. This may point to reduced reliability of regularized networks with low λ, yet the impact of the decreased sample size is unknown. A larger, well-balanced sample would be preferable to allow for diagnostic subgroup analysis.

Conclusion

Here, we provide strong evidence for impaired functioning within sensory brain networks in schizophrenia, as outlined by reduced SD in signal amplitude in visual, auditory, and sensorimotor nodes. Connectivity alterations were particularly strong among sensorimotor nodes, indicating reduced connectivity within sensorimotor nodes and alterations in their connections to the thalamus and brain networks supporting higher-order cognitive functions. The consistency to which sensorimotor nodes stood out across a range of analyses (SDSA, FC) and network estimation procedures (full correlations, [regularized] partial correlations) supports that sensorimotor networks are disrupted in schizophrenia. Thus, shifting future research focus from the cognitive to the sensory domain may enhance our understanding of schizophrenia pathophysiology.[40]

Supplementary Material

Supplementary material is available at http://schizophreniabulletin.oxfordjournals.org.

Funding

Research Council of Norway (#213837, #223273, #204966/F20); South-Eastern Norway Regional Health Authority (#2013-123, #2014-097); KG Jebsen Foundation. European Community's 7th Framework Progamme (#602450, IMAGEMEND).

Acknowledgments

The authors would like to thank the participants of the study for their contribution and the clinicians who were involved in patient recruitment and clinical assessments. Parts of the analysis was performed on the Abel Cluster, owned by the University of Oslo and the Norwegian metacenter for High Performance Computing (NOTUR), and operated by the Department for Research Computing at the University of Oslo IT department. The authors declare no conflict of interest.

References

1. WHO. *The Global Burden of Disease: 2004 Update*. Geneva, Switzerland: WHO Press; 2008.
2. Andreasen NC. A unitary model of schizophrenia: Bleuler's "fragmented phrene" as schizencephaly. *Arch Gen Psychiatry*. 1999;56:781–787.

3. Insel TR. Rethinking schizophrenia. *Nature*. 2010;468:187–193.
4. Friston KJ, Frith CD. Schizophrenia: a disconnection syndrome? *Clin Neurosci*. 1995;3:89–97.
5. McGuire PK, Frith CD. Disordered functional connectivity in schizophrenia. *Psychol Med*. 1996;26:663–667.
6. Pettersson-Yeo W, Allen P, Benetti S, McGuire P, Mechelli A. Dysconnectivity in schizophrenia: where are we now? *Neurosci Biobehav Rev*. 2011;35:1110–1124.
7. Lynall ME, Bassett DS, Kerwin R, et al. Functional connectivity and brain networks in schizophrenia. *J Neurosci*. 2010;30:9477–9487.
8. Green MF. Cognitive impairment and functional outcome in schizophrenia and bipolar disorder. *J Clin Psychiatry*. 2006;67:3–8.
9. Kahn RS, Keefe RSE. Schizophrenia is a cognitive illness: time for a change in focus. *JAMA Psychiatry*. 2013;70:1107–1112.
10. Javitt DC. Sensory processing in schizophrenia: neither simple nor intact. *Schizophr Bull*. 2009;35:1059–1064.
11. Hugdahl K. "Hearing voices": auditory hallucinations as failure of top-down control of bottom-up perceptual processes. *Scand J Psychol*. 2009;50:553–560.
12. Garrett DD, Kovacevic N, McIntosh AR, Grady CL. Blood oxygen level-dependent signal variability is more than just noise. *J Neurosci*. 2010;30:4914–4921.
13. Garrett DD, Kovacevic N, McIntosh AR, Grady CL. The importance of being variable. *J Neurosci*. 2011;31:4496–4503.
14. Yang GJ, Murray JD, Repovs G, et al. Altered global brain signal in schizophrenia. *Proc Natl Acad Sci U S A*. 2014;111:7438–7443.
15. Smith SM, Jenkinson M, Woolrich MW, et al. Advances in functional and structural MR image analysis and implementation as FSL. *Neuroimage*. 2004;23(suppl 1):S208–S219.
16. Jenkinson M, Bannister P, Brady M, Smith S. Improved optimization for the robust and accurate linear registration and motion correction of brain images. *Neuroimage*. 2002;17:825–841.
17. Beckmann CF, Smith SM. Probabilistic independent component analysis for functional magnetic resonance imaging. *IEEE Trans Med Imaging*. 2004;23:137–152.
18. Salimi-Khorshidi G, Douaud G, Beckmann CF, Glasser MF, Griffanti L, Smith SM. Automatic denoising of functional MRI data: combining independent component analysis and hierarchical fusion of classifiers. *Neuroimage*. 2014;90:449–468.
19. Pruim RHR, Mennes M, Buitelaar JK, Beckmann CF. Evaluation of ICA-AROMA and alternative strategies for motion artifact removal in resting state fMRI. *Neuroimage*. 2015;112:278–287.
20. Fischl B, Salat DH, Busa E, et al. Whole brain segmentation: automated labeling of neuroanatomical structures in the human brain. *Neuron*. 2002;33:341–355.
21. Jenkinson M, Smith S. A global optimisation method for robust affine registration of brain images. *Med Image Anal*. 2001;5:143–156.
22. Greve DN, Fischl B. Accurate and robust brain image alignment using boundary-based registration. *Neuroimage*. 2009;48:63–72.
23. Andersson JLR, Jenkinson M, Smith S. *Non-Linear Registration, aka Spatial Normalisation*. FMRIB Technial Report TR07JA2; 2010.
24. Filippini N, MacIntosh BJ, Hough MG, et al. Distinct patterns of brain activity in young carriers of the APOE-epsilon4 allele. *Proc Natl Acad Sci U S A*. 2009;106:7209–7214.
25. Smith SM, Miller KL, Salimi-Khorshidi G, et al. Network modelling methods for FMRI. *Neuroimage*. 2011;54:875–891.
26. Friedman JH. Regularized Discriminant-Analysis. *J Am Stat Assoc*. 1989;84:165–175.
27. Schäfer J, Strimmer K. A shrinkage approach to large-scale covariance matrix estimation and implications for functional genomics. *Stat Appl Genet Mol Biol*. 2005;4:Article32.
28. Baldi P, Brunak S, Chauvin Y, Andersen CA, Nielsen H. Assessing the accuracy of prediction algorithms for classification: an overview. *Bioinformatics*. 2000;16:412–424.
29. Matthews BW. Comparison of the predicted and observed secondary structure of T4 phage lysozyme. *Biochim Biophys Acta*. 1975;405:442–451.
30. Radmacher MD, McShane LM, Simon R. A paradigm for class prediction using gene expression profiles. *J Comput Biol*. 2002;9:505–511.
31. Nichols T, Hayasaka S. Controlling the familywise error rate in functional neuroimaging: a comparative review. *Stat Methods Med Res*. 2003;12:419–446.
32. Nichols T. FDR Implementation Provided Online by Tom Nichols. 2009. http://www-personal.umich.edu/~nichols/FDR/. Accessed April 27, 2015.
33. Power JD, Barnes KA, Snyder AZ, Schlaggar BL, Petersen SE. Spurious but systematic correlations in functional connectivity MRI networks arise from subject motion. *Neuroimage*. 2012;59:2142–2154.
34. Spence SA. Cognitive neurobiology of volition and agency in schizophrenia. In: Ron MA, Robbins TW, eds. *Disorders of Brain and Mind 2*. Cambridge, UK: Cambridge University Press; 2003:223–242.
35. Docx L, Morrens M, Bervoets C, et al. Parsing the components of the psychomotor syndrome in schizophrenia. *Acta Psychiatr Scand*. 2012;126:256–265.
36. Peralta V, Campos MS, De Jalón EG, Cuesta MJ. Motor behavior abnormalities in drug-naïve patients with schizophrenia spectrum disorders. *Mov Disord*. 2010;25:1068–1076.
37. Glahn DC, Laird AR, Ellison-Wright I, et al. Meta-analysis of gray matter anomalies in schizophrenia: application of anatomic likelihood estimation and network analysis. *Biol Psychiatry*. 2008;64:774–781.
38. Li HJ, Xu Y, Zhang KR, Hoptman MJ, Zuo XN. Homotopic connectivity in drug-naive, first-episode, early-onset schizophrenia. *J Child Psychol Psychiatry*. 2014;56:432–443.
39. Butler PD, Javitt DC. Early-stage visual processing deficits in schizophrenia. *Curr Opin Psychiatry*. 2005;18:151–157.
40. Javitt DC, Freedman R. Sensory processing dysfunction in the personal experience and neuronal machinery of schizophrenia. *Am J Psychiatry*. 2015;172:17–31.
41. Andreasen NC. The role of the thalamus in schizophrenia. *Can J Psychiatry*. 1997;42:27–33.
42. Cronenwett WJ, Csernansky J. Thalamic pathology in schizophrenia. *Curr Top Behav Neurosci*. 2010;4:509–528.
43. Anticevic A, Cole MW, Repovs G, et al. Characterizing thalamo-cortical disturbances in schizophrenia and bipolar illness. *Cereb Cortex*. 2014;24:3116–3130.
44. Woodward ND, Karbasforoushan H, Heckers S. Thalamocortical dysconnectivity in schizophrenia. *Am J Psychiatry*. 2012;169:1092–1099.
45. Fair DA, Bathula D, Mills KL, et al. Maturing thalamocortical functional connectivity across development. *Front Syst Neurosci*. 2010;4:10.
46. McIntosh AR, Kovacevic N, Lippe S, Garrett D, Grady C, Jirsa V. The development of a noisy brain. *Arch Ital Biol*. 2010;148:323–337.

47. Fox MD, Snyder AZ, Zacks JM, Raichle ME. Coherent spontaneous activity accounts for trial-to-trial variability in human evoked brain responses. *Nat Neurosci*. 2006;9:23–25.
48. Nir Y, Mukamel R, Dinstein I, et al. Interhemispheric correlations of slow spontaneous neuronal fluctuations revealed in human sensory cortex. *Nat Neurosci*. 2008;11:1100–1108.
49. Cuthbert BN, Insel TR. Toward the future of psychiatric diagnosis: the seven pillars of RDoC. *BMC Med*. 2013;11:126.
50. Alnæs D, Kaufmann T, Richard G, et al. Attentional load modulates large-scale functional brain connectivity beyond the core attention networks. *Neuroimage*. 2015;109:260–272.
51. Smith SM, Miller KL, Moeller S, et al. Temporally-independent functional modes of spontaneous brain activity. *Proc Natl Acad Sci U S A*. 2012;109:3131–3136.
52. Schürmann M, Järveläinen J, Avikainen S, et al. Manifest disease and motor cortex reactivity in twins discordant for schizophrenia. *Br J Psychiatry*. 2007;191:178–179.